



Synthesis and vibrational spectral (FT-IR, FT-Raman) studies, NLO properties & NBO analysis of (E)-N'(thiophen-2yl methylene)isonicotinohydrazide using quantum chemical method

A. Nathiya¹, H. Saleem^{1*}, S. Bharanidharan², M. Suresh³

¹Department of Physics, Annamalai University, Annamalainagar-608 002, Tamil Nadu, India

²Department of Physics, Bharath Institute of Higher Education and Research, Bharath University, Chennai-600 073, Tamil Nadu, India

³Department of Chemistry, College of Engineering, Guindy, Anna University, Chennai-620 025, Tamil Nadu, India

*Corresponding author E-mail: saleem_h2001@yahoo.com

Abstract

FT-IR (4000-400 cm⁻¹) and FT-Raman (3500-50 cm⁻¹) spectra of (E)-N'(thiophen-2yl methylene)isonicotinohydrazide (TMINH) molecule was recorded in solid phase. The optimized geometry was calculated by B3LYP method with 6-311++G(d,p) basis set. The harmonic vibrational frequencies, infrared (IR) intensities and Raman scattering activities of the title compound were performed at same level of theory. The complete vibrational assignments were performed on the basis of the Total energy distribution (TED) of the vibrational modes, calculated with scaled quantum mechanical (SQM) method. The calculated first hyperpolarizability may be attractive for further studies on non-linear optical (NLO) properties of material. Stability of the molecule arising from hyperconjugative interaction and charge delocalization was analyzed using natural bond orbital (NBO) analysis. Highest occupied molecular orbital-Lowest unoccupied molecular orbital (HOMO-LUMO) energy gap explains the eventual charge transfer interactions taking place within the title molecule. A study on the electronic properties, such as excitation energies and wavelengths, were performed by time-dependent (TD-DFT) approach. Molecular electrostatic potential (MEP) provides the information on the electrophilic, nucleophilic and free radical prone reactive sites of the molecule. The thermodynamic properties such as heat capacity, entropy and enthalpy of the title compound were calculated at different temperatures in gas phase. ¹H and ¹³C-NMR chemical shifts of the molecule were calculated using Gauge-independent atomic orbital (GIAO) method. To establish information about the interactions between human cytochrome protein and this novel compound theoretically, docking studies were carried out using Schrödinger software.

Keywords: FT-IR; FT-Raman; NBO; HOMO-LUMO; Molecular Docking.

1. Introduction

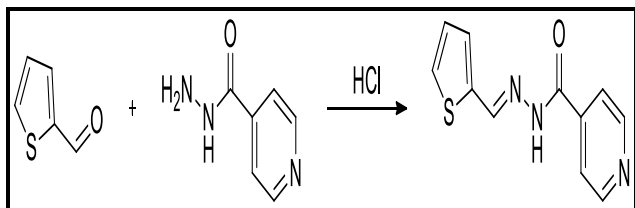
The use of computational techniques is becoming increasingly common throughout all the various fields physics and chemistry and biology (Davidson, 2000). Especially, thiophene derivatives have been reported to possess broad spectrum of biological properties including anti-inflammatory, analgesic, anti-depressant, anti-microbial and anti-convulsant activities (Molvi et al., 2007; SatheeshaRai et al., 2008; Ashalatha et al., 2007). Now, presently available active anti-epileptic drugs like tiagabine, etizolam, brotizolam are containing thiophene moiety in their structures as active pharmacophore (Polivka et al., 1984; Noguchi et al., 2004). Thiophene-containing compounds are known as materials with potential applications in the flavor (Guentert et al., 2010) and pharmaceutical industries (Press, 1991), in conducting polymer design (Bloor, 1995), as well as in NLO materials (Nalwa, 1993). Thiophene derivatives are also often used as intermediates in a wide range of areas of synthetic chemistry. The insertion of thiophene in the linear ethynyl-phenyl conjugated chain, gives a

higher electron delocalization to the molecule (Wu et al., 1999). Hydrazides, carbohydrazides and similar compounds are well known as useful building blocks for the synthesis of a variety of heterocyclic rings. A large number of heterocyclic carbohydrazides and their derivatives are reported to exhibit significant biological activities (Mansour et al., 2003; Metwally et al., 2006) and the carbohydrazide function represents an important pharmacophoric group in several classes of therapeutically useful substances (Mansour et al., 2003; Ghiglieri-Bertez et al., 1987). In this study, the TMINH molecule was synthesized and characterized by FT-IR and FT-Raman spectral analysis. The vibrational assignments were made with the aid of TED. The NLO activity as well as the NBO study for TMINH molecule were performed to get more precise information about the hybridization and hydrogen bonding interaction of orbitals energies. The HOMO-LUMO energy gap was calculated to give more information about the charge transfer within the molecule. Information about the size, shape, charge density distribution and site of chemical reactivity of TMINH were obtained by mapping electron density (ED) isosurface with MEP surfaces.

2. Experimental details

2.1. Synthesis procedure

A mixture of Thiophene-2-carboxaldehyde (2.1mL, 0.01mol) and isonicotinic acid hydrazide (1.37g, 0.01mol) in 5 mL of ethanol was stirred in the presence of 2 drops of concentrated HCl for one hour. The reaction mixture was maintained at room temperature and the colourless solid was obtained. The solid was separated and filtered under suction, washed with ice-cold water (50ml). The precipitate was washed with water and filtered and again washed with petroleum ether (40–60%) and dried over in a vacuum desiccator then the product was recrystallized from hot ethanol.



2.2. FT-IR, FT-Raman, NMR and UV-Vis. spectra details

The FT-IR spectrum was recorded in the spectral range 4000-400 cm^{-1} using KBr pellet technique with a FT-IR-Shimadzu spectrometer. The spectrum was recorded at room temperature with a scanning speed of 10 cm^{-1} per minute with the spectral resolution of 2.0 cm^{-1} at Instrumentation laboratory, Jamal Mohamed College, Tiruchirappalli, Tamilnadu. FT-Raman spectrum was observed using laser source Nd:YAG 1064 nm as excitation wavelength in the region 50-4000 cm^{-1} on Bruker IFS 66v spectrophotometer equipped with a FRA 106 FT-Raman module accessory and at spectral resolution of 4 cm^{-1} . The FT-Raman spectrum was recorded at SAIF Laboratory, IIT Madras. The UV-Vis absorption spectrum of TMINH was recorded in the range of 200-500 nm using a Shimadzu-2600 spectrometer in the department of Chemistry, Jamal Mohamed College, Tiruchirappalli, Tamilnadu. ^1H NMR spectra were recorded on a Bruker 400 MHz spectrometer and ^{13}C NMR spectra were recorded on a Bruker 100 MHz spectrometer in the department of chemistry, Annamalai University, Annamalai Nagar. Chemical shift values are reported in parts per million (ppm) and Tetramethylsilane (TMS) as internal standard.

2.3. Computational methods

The entire quantum chemical calculations were performed by DFT (B3LYP) method using Gaussian 03W program package (Gaussian 03 Program, 2004; Frisch et al., 2004). The optimized structural parameters and vibrational frequencies were calculated. The TED analysis was made to using VEDA4 program (Jamroz, 2004). The vibrational frequency assignments were made with a high degree of accuracy. The NBO calculations were performed using NBO 3.1 program (Glendening et al., 1998) as implemented in the Gaussian 03W (Gaussian 03 Program, 2004; Frisch et al., 2004) package. In the present work, the DFT approach with 6-311++G(d,p) as basis set for computation of molecular structure, vibrational frequencies and energies of optimized structures was utilized. The Bond parameters, NLO, NBO, HOMO-LUMO, UV, Mulliken charges, MEP, thermodynamic parameters and NMR chemical shift are calculated using B3LYP method with 6-311++G(d,p) basis set.

2.4. Molecular docking study

In this study, the molecular docking study was performed in Dell workstation equipped with Xeon processor E3-1225, 3.20 GHz, V2 quadcore personal computer with 8 GB total RAM and with Schrödinger software suite, 2014-4 release, LLC, New York.

Initially, the structure of TMINH and protein were optimized and minimized before docking program. The 3D crystal structure of lanosterol 14-alpha dimethylase (PDB ID: 3LD6) was downloaded from protein data bank (www.rcsb.com). The structure of protein complex was optimized and minimized in protein preparation wizard (Epik Version 2.3, Schrödinger, 2014) using Optimized Potential for Liquid Simulations (OPLS-2005) force field (Jorgensen et al., 1996) until the root mean square deviation (RMSD) reached the value of 0.3Å. The protein grid was generated using Glide (Glide Version 5.8, Schrödinger, 2014) module which is incorporated in Maestro (Maestro, Schrödinger, 2014) applications. Later, the 2D structure of compound was optimized; minimized and possible conformers were generated using Ligprep (Ligprep, Version 2.5, Schrödinger, 2014) module of Schrödinger software. The binding mode interactions of the tested compounds with 2YP3 were identified by the extra precision (XP) mode of docking using Glide module.

3. Results and discussion

3.1. Geometrical parameters

The optimized parameters such as bond lengths, bond angles and dihedral angles values are listed in Table 1 and the atom numbering scheme is shown in Fig. 1. The $\text{C}_1=\text{C}_2$, $\text{C}_3=\text{C}_4$, C_1-S_5 and C_4-S_5 calculated bond lengths are: 1.3676, 1.3779, 1.7316 & 1.7480 Å, in which the shortening of bond lengths ($\text{C}_3=\text{C}_4$ & C_4-C_5) are due to the attachment of hydrazone moiety at C_4 atom and hence the calculated bond angle of $\text{C}_3-\text{C}_4-\text{S}_5$ (110.85°) is also expected to be shorter than the $\text{C}_2-\text{C}_1-\text{S}_5$ (112.27°) bond angle. This trend is supported by our earlier study and also find support from literature (Balachandran et al., 2014; Fleming et al., 2006). The thiophene and hydrazone moieties of TMINH are co-planar as it is evident from the dihedral angles $\text{C}_3-\text{C}_4-\text{C}_9-\text{N}_{12}/\text{S}_5-\text{C}_4-\text{C}_9-\text{N}_{12}$ and $\text{C}_3-\text{C}_4-\text{C}_9-\text{H}_{10}/\text{S}_5-\text{C}_4-\text{C}_9-\text{H}_{10}$ are $179.12^\circ/-0.94^\circ$ and $-1.07^\circ/178.87^\circ$, respectively and also there is a good conjugation between p-orbitals of all atoms of hydrazone and thiophene moieties. The bond angle of $\text{C}_{16}-\text{C}_{14}-\text{O}_{15}$: 121.53° is positively $\sim 2.99^\circ$ deviated from $\text{N}_{11}-\text{C}_{14}-\text{O}_{15}$: 118.54° , which is due to the presence of two electronegativity atoms (N_{11} & O_{15}) next to C_{14} and their electronegativities are in the order: $\text{O} > \text{N} > \text{C}$. Most of the calculated bond parameters are comparable with our previous study T2CNH and also find support from the XRD values (Song and Fan, 2009).

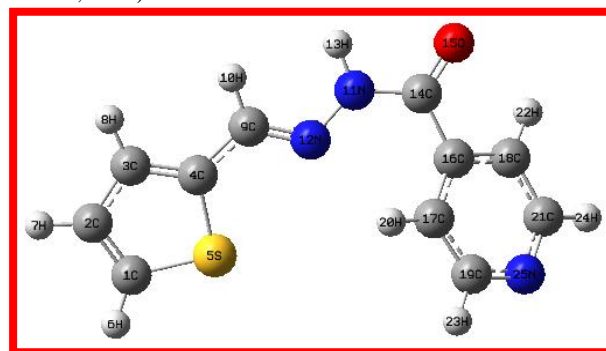


Fig. 1: The Optimized Molecular Structure of TMINH.

Table 1: The Selected Bond Parameters of TMINH Using B3LYP/6-311++G(d,p)

Bond Parameters Bond Lengths (Å)	B3LYP/6-311++G(d,p)	XRD data*
C1-C2	1.3676	1.377
C1-S5	1.7316	1.7185
C1-H6	1.0795	0.95
C2-C3	1.4204	1.434
C2-H7	1.0817	0.95
C3-C4	1.3779	1.375
C3-H8	1.0827	0.95
C4-S5	1.7480	1.704
C9-N12	1.2836	1.287
N11-N12	1.358	1.3856
N11-H13	1.0196	0.88
N11-C14	1.3826	1.3572
C14-O15	1.2203	1.2295
Bond Angles (°)		
C2-C1-S5	112.27	111.1
C2-C1-H6	128.16	124.4
S5-C1-H6	119.57	124.4
S5-C4-C9	122.73	121.64
N12-N11-H13	120.12	119.3
N12-N11-C14	125.22	119.96
H13-N11-C14	113.75	120.4
C19-N25-C21	117.13	116.86
Dihedral Angles (°)		
S5-C1-C2-C3	-0.10	0.19
S5-C1-C2-H7	179.88	
C2-C1-S5-C4	0.14	-0.19
H6-C1-S5-C4	179.97	
C1-C2-C3-C4	-0.00	0.39
C2-C3-C4-S5	0.11	-0.8
C2-C3-C4-C9	-179.94	-178.99
C3-C4-S5-C1	-0.14	-0.78
C9-C4-S5-C1	179.91	178.62
C3-C4-C9-H10	-1.07	
C3-C4-C9-N12	179.12	177.64
S5-C4-C9-H10	178.87	
S5-C4-C9-N12	-0.94	
C4-C9-N12-N11	179.90	179.34
H10-C9-N12-N11	0.10	
H13-N11-N12-C9	-5.32	
C14-N11-N12-C9	-173.78	175.8
N12-N11-C14-O15	168.95	3.7

* Song, M.Z., Fan, C.G., Acta. Cryst. E 65 (2009) o2800.

3.2. Vibrational assignments

The TMINH molecule has 25 atoms and belongs to C_1 point group symmetry, hence 69 normal modes of vibrations are possible and are distributed as $\Gamma_{\text{vib}} = 47A' + 22A''$. All the vibrations are active in both IR and Raman absorption. The exclusion of anharmonicity factor and the level of basis set used, certain theoretical frequencies are not matched with that of experimental values. Hence, in this study, a linear scaling procedure is used to scale down the harmonic frequencies; we have followed the uniform scaling factor 0.9608 for DFT method (Rauhut and Pulay, 1995). After scaling the calculated frequencies, the deviation from the observed values are less than 10 cm^{-1} with few exceptions. The scaled frequencies, observed frequencies (FTIR, FT-Raman) with their intensities, force constants, reduced masses and proposed vibrational assignments along with TED values are listed in Table 2. The simulated, observed FTIR and FT-Raman spectra are shown in Figs. 2 and 3, respectively.

3.2.1. CH vibrations

The hetero aromatic organic compounds commonly exhibit multiple bands in the region of $3000\text{-}3100 \text{ cm}^{-1}$ due to CH stretching vibrations (Nagabalasubramanian et al., 2012). In this study, there are four hydrogen atom surrounded by pyridine ring hence four CH stretching vibrations are possible. The bands observed at 3090 cm^{-1} as weak band in FT-Raman and at 3027 cm^{-1} as medium band in FTIR spectra are designated as ν_{CH} mode of pyridine moiety, while the calculated frequencies are in the

range of $3029, 3033, 3079$ and 3099 cm^{-1} (mode nos: 62, 63, 65, 67). These assignments are coincide well with literature (Krishnakumar et al., 2005) and also find support from their TED value.

In general, the CH in-plane bending vibrations normally occur as number of strong and weak bands in the region $1000\text{-}1400 \text{ cm}^{-1}$ (Sundaraganesan et al., 2005). Similarly, the CH out-of-plane bending vibrations are expected in the region of $809\text{-}950 \text{ cm}^{-1}$ (Singh and Pandey, 1974). In this work, the CH in-plane bending vibrations of pyridine are assigned at 1291 (m), 1363 (w) cm^{-1} in FTIR spectrum and 1082 (w), 1299 (s), 1367 (w) cm^{-1} in FT-Raman spectrum and their related harmonic frequencies are: $1195, 1300, 1382, 1462 \text{ cm}^{-1}$ (mode nos: 44, 49, 52, 55). The pyridine CH out-of-plane bending vibration of TMINH molecule observed at $847, 935 \text{ cm}^{-1}$ as weak, medium bands in FTIR spectrum, while the Raman bands are missing. For the same mode, the calculated frequencies are: $824, 856, 946$ & 963 cm^{-1} (mode nos: 30, 32, 35, 36). These assignments are in agreement with above literature values and also find support from TED values.

3.2.2. Thiophene ring

In general, thiophene ring CH stretching vibrations are expected to appear in the wavenumber region $3000\text{-}3100 \text{ cm}^{-1}$ with multiple weak bands (Varsanyi, 1973; Jag, 2001). The CH in-plane/out-of-plane bending vibrations are respectively appearing in the regions of $1100\text{-}1500/800\text{-}1000 \text{ cm}^{-1}$. These bands are not sensitive to the nature of substituents (Jag, 2001). The calculated frequencies ($3070, 3086, 3116 \text{ cm}^{-1}$ /mode nos: 64, 66, 68) and observed FT-Raman band (3067 cm^{-1}) are assigned to ν_{CH} modes of

thiophene. These assignments are in agreement with literature and are further supported by TED values (>92%). Similarly, the harmonic frequencies: 1026, 1063, 1198 cm^{-1} mode nos: 38, 40, 45 and 685, 800, 881 cm^{-1} /mode nos: 24, 29, 33 are attributed to β_{CH} and Γ_{CH} modes of thiophene, respectively. These assignments are agreeable with above literature and also find supported from observed FT-Raman band: 1061 cm^{-1} in addition to TED values (>28%, 24%).

3.2.3. Hydrazone moiety

In hydrazone linkage, the harmonic frequencies for ν_{CH} , β_{CH} , Γ_{CH} modes were assigned at 2901, 1335, 908 cm^{-1} , respectively (Bharanidharan et al., 2017) and these assignments are in close agreement with the present assignments: $\nu_{\text{CH}}/2917$, $\beta_{\text{CH}}/1335$, $\Gamma_{\text{CH}}/909$ cm^{-1} (mode nos: 61, 51, 34). The mode no: 40 (1063/FT-Raman: 1061 cm^{-1}) having TED value: 46% is attributed to $\beta_{\text{S}_5\text{C}_1\text{H}_6}$ mode.

The ν_{CH} , β_{CH} and Γ_{CH} vibrations of pyridine moiety in (E)-N'-Thiophen-2-yl methylene) nicotinothiazide (T2CNH) were assigned in the regions of 3016-3076, 1173-1447 and 808-974 cm^{-1} (Jag, 2001). Similarly, for thiophene ring, the above modes were assigned in the ranges of 3078-3120, 1015-1219 and 817-819 cm^{-1} , respectively. It should be mentioned here that the ν_{CH} , β_{CH} , Γ_{CH} modes of pyridine/thiophene rings of TMINH are positively deviated from literature (Bharanidharan et al., 2017), since the hydrazone linkage is fused with pyridine ring in the para position.

3.2.4. C=O vibrations

The multiple bonded group is highly polar (C=O) and therefore it gives rise to an intense IR absorption band. The carbon-oxygen double bond is formed by $\pi\text{-}\pi$ bonding between carbon and oxygen atoms. The lone pair of electron in oxygen also determines the nature of the carbonyl group (Sathyanarayanan, 2004). The carbonyl group C=O stretching wave number shifts to a lower value typically absorbs very strongly in the range 1660-1715 cm^{-1} (Roeges, 1994; Barthes et al., 1996; James et al., 2008). In the present investigation, a very strong band appeared at 1666 cm^{-1} in FTIR and a medium intense band observed at 1664 cm^{-1} in FT-Raman spectrum, which shows the presence of carbonyl group (C=O) in the present molecule. This assignment is in line with the harmonic frequency (1660 cm^{-1} /mode no: 60) with 78% of TED value and also find support from the literature values (Roeges, 1994; Barthes et al., 1996; James et al., 2008).

The $\beta_{\text{C=O}}/\Gamma_{\text{C=O}}$ vibrations are assigned to mode nos: 22, 17, 12/30, 27, 25, respectively and are also contaminated by β_{CC} and Γ_{HCC} modes, respectively. It should be mentioned here that the $\Gamma_{\text{C=O}}$ mode appear at higher frequency than the $\beta_{\text{C=O}}$, which may be due to lone pair electrons of nitrogen. The present assignment ($\nu_{\text{C}_{14}=\text{O}_{15}}$) is negatively (~ 5 cm^{-1}) deviated from literature (Bharanidharan et al., 2017), while the harmonic frequency is also negatively (28 cm^{-1}) deviated. This may be due to the hydrazone moiety is fused in the fourth position of pyridine ring (i.e, para position).

3.2.5. C-S vibrations

In this study, the mode nos: 23 and 26 are ascribed to $\nu_{\text{C}_4\text{-S}_5}/679$ cm^{-1} and $\nu_{\text{C}_1\text{-S}_5}/719$ cm^{-1} modes, respectively in accordance with the literature (Singh et al., 2008; Fleming et al., 2006). This mode is well known to mixed with neighbouring modes: β_{CC} thiophene (Badawi, 2009). This assignment is justified by observed 681 cm^{-1} (FTIR) band and also find support from TED value (>33%). The harmonic frequencies 609, 661 and 491, 560 cm^{-1} (mode nos: 20, 22 and 16, 18) are designated as β_{CCS} and Γ_{CCS} modes, respectively. These assignments having considerable TED values and also find support from the observed FTIR: 506 cm^{-1} band.

It should be discussing here that the present assignment $\nu_{\text{C}_4\text{-S}_5}/679$ cm^{-1} is negatively deviated (112 cm^{-1}) from the literature (791 cm^{-1} : $\nu_{\text{C}_1\text{-S}_5}$), which may be due to unhybridized

orbital of sulphur containing two electrons form part of the delocalized electron cloud by lateral overlapping with unhybridized orbital of carbon atoms. Electron pair in one of the hybrid orbital remains shared.

3.2.6. C-C vibrations

Literature survey revealed that the C-C vibrations of thiophene ring were assigned in the ranges of 1329-1431, 1420-1501 and 1419-1519 cm^{-1} (Lorenc, 2012). The C-C stretching modes of the thiophene ring have been observed at 1415/1513 cm^{-1} in FTIR/FT-Raman spectra and their corresponding calculated frequencies are 1404, 1507 cm^{-1} (mode nos: 53, 56). These assignments are within the frequency range and also find support from literature (Bharanidharan et al., 2017) in addition to TED values (55, 40%). The $\nu_{\text{C}_2=\text{C}_1}$ mode observed at higher frequency (1513 cm^{-1}) than $\nu_{\text{C}_3=\text{C}_4}$, since the hydrazone moiety is attached with C_4 atom. It is evident from the Table 2, these modes are not pure modes and they mixed with β_{CCH} mode. Further, the harmonic frequency at 1026 cm^{-1} (mode no: 38) with TED 44% is assigned to $\nu_{\text{C}_3-\text{C}_2}$ of thiophene ring. The bands arising from β_{CC} and Γ_{CC} modes of thiophene moiety are assigned to harmonic bands identified at 719, 835 cm^{-1} (mode nos: 26, 31) and 131, 322 cm^{-1} (mode nos: 6, 11), respectively. These assignments find support from the above literature.

In pyridine ring, the carbon-carbon stretching vibrations were reported in the ranges of 1590-1640, 1560-1580 and 1470-1510 cm^{-1} (Lorenc, 2012). The C-C modes were assigned at 1549 cm^{-1} /FTIR and at 1195, 1241 cm^{-1} /FT-Raman. Based on the above facts, the observed bands: 1217/1222 (m); 1363 (w), 1574 (s) cm^{-1} are designated as $\nu_{\text{C-C}}$ modes of pyridine ring. These assignments find support from the harmonic wavenumber: 1225, 1382, 1531, 1568 cm^{-1} (mode nos: 47, 52, 57, 58) and also from TED values. The $\beta_{\text{C}_{18}\text{C}_{21}\text{N}_{25}}/\beta_{\text{C}_{17}\text{C}_{19}\text{N}_{25}}$, $\beta_{\text{C}_{21}\text{N}_{25}\text{C}_{19}}$ and $\beta_{\text{C}_{16}\text{C}_{14}\text{N}_{11}}$, $\beta_{\text{N}_{12}\text{C}_9\text{C}_4}$, $\beta_{\text{N}_{11}\text{N}_{12}\text{C}_9}$ deformations of pyridine and hydrazone moieties, respectively assigned to 1050/973, 973 and 609, 661, 771 cm^{-1} (mode nos: 39/37, 37 and 20, 22, 28). Similarly, $\Gamma_{\text{N}_{25}\text{C}_{19}\text{C}_{21}\text{C}_{18}}$, $\Gamma_{\text{C}_{21}\text{C}_{18}\text{N}_{25}\text{C}_{16}}$ and $\tau_{\text{C}_{18}\text{C}_{16}\text{C}_{14}\text{N}_{11}}$ modes are ascribed to wavenumbers: 469, 735, 68 cm^{-1} (mode nos: 15, 27, 4). These assignments having considerable TED values. The mode nos: 50/45 are attributed to $\nu_{\text{C}_{16}-\text{C}_{14}}/\nu_{\text{C}_4-\text{C}_9}$ modes, in which mode no: 50 is in agreement with observed FT-Raman band/1321 cm^{-1} . From literature (Bharanidharan et al., 2017), the same modes were assigned at 1215 cm^{-1} (harmonic)/1096 cm^{-1} (FT-Raman) in the case of T2CNH. The positive deviation (~ 100 cm^{-1}) of wavenumbers which may be due to conjugation of the carbonyl group attached to the fourth position of pyridine ring.

3.2.7. C=N, C-N vibrations

In this study, the hydrazone linkage fuses the thiophene and pyridine rings, which leads the vibrations such as $\nu_{\text{C=N}}$, $\nu_{\text{C-N}}$ as well as deformation modes. The C=N stretching vibration appears in the region of 1600-1670 cm^{-1} (Socrates, 1980; Subashchandrabose et al., 2013). In hydrazone moiety, the $\nu_{\text{C}_9=\text{N}_{12}}$ mode assigned to strong band: 1595 cm^{-1} observed in FT-Raman spectrum, while the FTIR counterpart is missing and its corresponding calculated value is 1594 cm^{-1} (mode no: 59). This assignment is supported by TED value (71%) in addition to literature (Bharanidharan et al., 2017). Silverstein et al., 1981 assigned CN stretching absorption in the region 1266-1382 cm^{-1} for aromatic amines. In another study T2CNH (Bharanidharan et al., 2017) the same mode was assigned at 1097 cm^{-1} /FT-Raman was designated as $\nu_{\text{C-N}}$ vibration and the value of this band was calculated at 1097 cm^{-1} with TED of 40%. In this study, the $\nu_{\text{C}_{14}-\text{N}_{11}}$ mode assigned to wavenumber 1086 cm^{-1} (mode no: 42). These assignments are positively ($\nu_{\text{C=N}}$: 6/ $\nu_{\text{C-N}}$: 10 cm^{-1}) deviated from T2CNH (Bharanidharan et al., 2017). This may be due to hydrazone moiety is attached with C_{16} atom of pyridine ring.

Literature survey revealed that the IR and Raman bands observed between 1515 and 1232 cm^{-1} have been assigned to $\nu\text{C-N}$ modes of pyridine, ring in the case of (E)-1-((Pyridine-2-yl) methylene) semicarbazide (Silverstein et al., 1981). From literature, the C-N modes were assigned at 1563: harmonic and 1241 cm^{-1} : FT-Raman in T2CNH (Bharanidharan et al., 2017). In this study, the $\nu\text{C-N}$ bands belong to pyridine moiety are recorded as mixed vibrations (with $\nu\text{C-C}$) at 1531 cm^{-1} /mode no: 57 (harmonic) and at 1217/1222 cm^{-1} (FTIR/FT-Raman), respectively. This assignment is negatively (32/19 cm^{-1}) deviated from our earlier assignments. This may be due to the hydrazone moiety is attached with para position of pyridine ring. The $\beta\text{C}_{16}\text{C}_{14}\text{N}_{11}$, $\beta\text{N}_{12}\text{C}_9\text{C}_4$ and $\beta\text{C}_{17}\text{C}_{19}\text{N}_{25}$, $\beta\text{C}_{18}\text{C}_{21}\text{N}_{25}$, $\beta\text{C}_{21}\text{N}_{25}\text{C}_{19}$ deformations belong to hydrazone and pyridine moieties, respectively assigned to wavenumbers: 609, 661 cm^{-1} (mode nos: 20, 22) and 1050, 973, 973 cm^{-1} (mode nos: 39, 37, 37). Similarly, $\tau\text{C}_{16}\text{C}_{14}\text{N}_{11}\text{N}_{12}$, $\tau\text{N}_{11}\text{N}_{12}\text{C}_9\text{C}_4$ and $\Gamma\text{N}_{25}\text{C}_{19}\text{C}_{21}\text{C}_{18}$, $\Gamma\text{C}_{14}\text{C}_{16}\text{C}_{18}\text{C}_{17}$ modes are assigned to wavenumbers: 245, 322 and 469, 469 cm^{-1} (mode nos: 9, 11, 15, 15).

3.2.8. N-N vibrations

The present molecule has one hydrazone moiety and hence the following vibrations are possible: ν_{NN} , β_{NN} & Γ_{NN} . In T2CNH, the harmonic frequency 1148 and observed frequencies 1145: FTIR/1149 cm^{-1} : FT-Raman were assigned to $\nu_{\text{N-N}}$ mode (Bharanidharan et al., 2017). In this study, the harmonic

wavenumber 1128 cm^{-1} is in moderate agreement with above literature, while the IR and Raman bands are missing. This negative ($\sim 20 \text{ cm}^{-1}$) deviation is mainly due to N-H part attached to the C=O group. The $\beta\text{N}_{11}\text{N}_{12}\text{C}_9$, $\beta\text{C}_{14}\text{N}_{11}\text{N}_{12}$ and $\tau\text{C}_{16}\text{C}_{14}\text{N}_{11}\text{N}_{12}$, $\tau\text{N}_{11}\text{N}_{12}\text{C}_9\text{C}_4$ modes are assigned to mode nos: 10, 8 and 9, 11, respectively.

3.2.9. N-H vibrations

In general, the $\nu\text{N-H}$ modes expected to occur in the region 3200-3400 cm^{-1} (Lorenz, 2012) and the same mode was assigned at 3367 cm^{-1} in FTIR spectrum (Bharanidharan et al., 2017). In agreement with these observations, the harmonic band 3333 cm^{-1} (mode no:69) is designated as $\nu\text{N-H}$ mode, while the experimental bands are missing. This mode is a pure mode (TED: 100%) and also find support from literature (Ramesh Babu et al., 2014). The harmonic wavenumber for $\beta\text{N}_{12}\text{N}_{11}\text{H}_{13}/\tau\text{H}_{13}\text{N}_{11}\text{N}_{12}\text{C}_9$ lies at 1449/578 cm^{-1} , respectively having considerable TED value (40/65%). As per the investigation of (Geskin et al., 2003) the $\beta\text{NH}/\Gamma\text{NH}$ modes appeared at 1475 (FT-Raman)/521 cm^{-1} (FTIR) in the case of (E)-N'-(furan-2yl) methylene) nicotinothiazide (F2CNH). From literature (Bharanidharan et al., 2017), the same modes were assigned at 1508/488 cm^{-1} . On comparing the present investigation with above literature, the lowering/increasing of wavenumbers may be due to delocalization of electrons in pyridine ring.

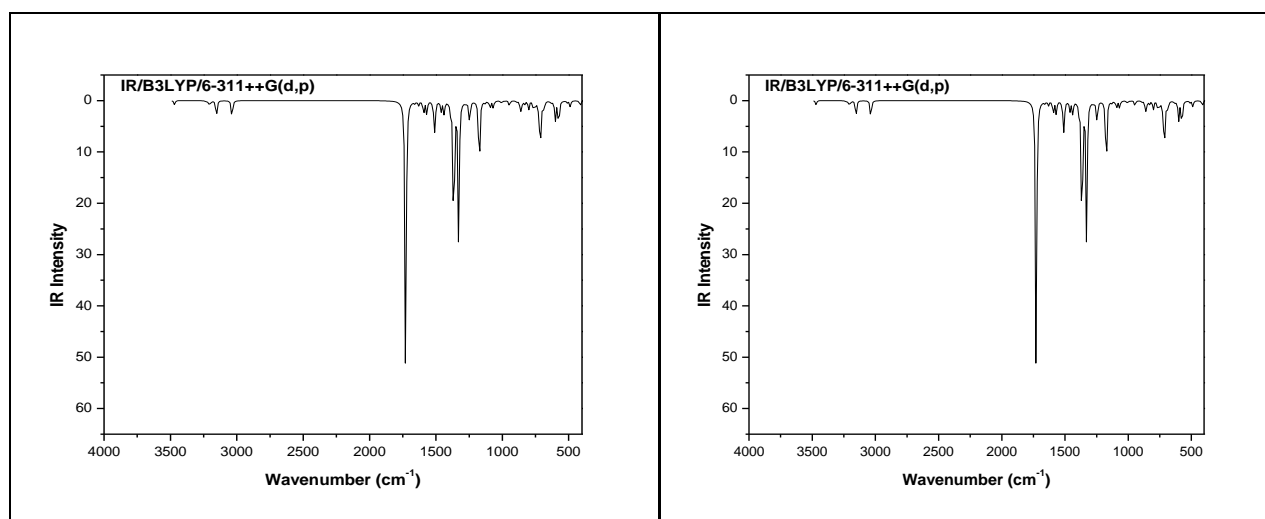


Fig. 2: The Combined Theoretical and Experimental IR Spectra of TMINH.

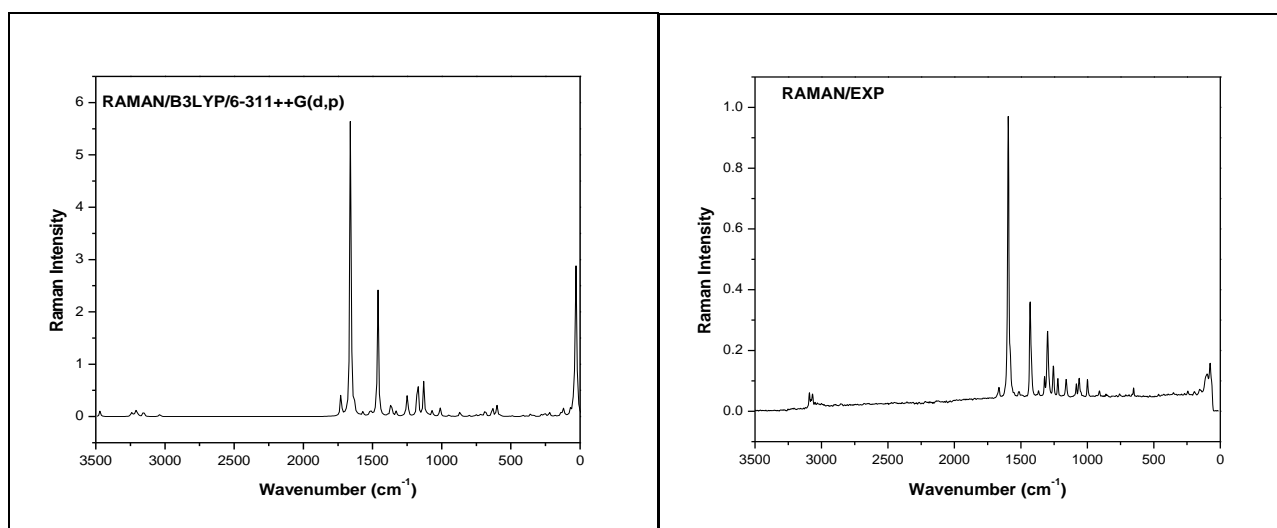


Fig. 3: The Combined Theoretical and Experimental FT-Raman Spectra of TMINH.

Table 2: The Experimental and Calculated Frequencies of TMINH Using B3LYP/6-311++G(d,p) Level of Basis Set [Harmonic Frequencies (cm⁻¹), IR, Raman Intensities (Km/Mol), Reduced Masses (amu) and Force Constants (Mdyna⁻¹)]

Mode No.	Calculated Frequencies (cm ⁻¹)		Observed Frequencies (cm ⁻¹)		IR Intensity Rel. ^b	Raman Intensity Rel. ^c	Reduced Masses	Force Constant	Vibrational Assignments \geq 10% (TED) ^d
	Un Scaled	Scaled ^a	FT-IR	FT-Raman					
1	28	27			0.03	100.00	4.89	0.00	β C ₁₄ N ₁₁ N ₁₂ (16)+ β C ₁₆ C ₁₄ N ₁₁ (13)+ τ C ₁₈ C ₁₆ C ₁₄ N ₁₁ (33)
2	32	31			0.09	40.97	6.64	0.00	τ C ₃ C ₄ C ₉ N ₁₂ (40)+ τ C ₁₄ N ₁₁ N ₁₂ C ₉ (29)
3	44	42			0.02	18.19	5.67	0.01	β N ₁₂ C ₉ C ₄ (16)+ β C ₉ N ₁₁ N ₁₂ (13)+ τ C ₁₄ N ₁₁ N ₁₂ C ₉ (10)+ τ C ₁₆ C ₁₄ N ₁₁ N ₁₂ (19)
4	71	68		76(m)	0.13	4.37	7.15	0.02	τ C ₁₈ C ₁₆ C ₁₄ N ₁₁ (35)+ τ N ₁₁ N ₁₂ C ₉ C ₄ (12)+ τ C ₂ C ₃ C ₄ C ₉ (10)
5	118	114			0.13	6.44	7.30	0.06	β N ₁₂ C ₉ C ₄ (10)+ β C ₉ C ₄ S ₅ (20)+ β C ₁₆ C ₁₄ N ₁₁ (17)+ Γ C ₁₄ C ₁₆ C ₁₈ C ₁₇ (25)
6	136	131			0.14	3.96	6.64	0.07	τ C ₃ C ₄ C ₉ N ₁₂ (23)+ C ₁₄ N ₁₁ N ₁₂ C ₉ (32)+ τ C ₂ C ₃ C ₄ C ₉ (19)
7	180	173			0.17	0.67	5.54	0.11	τ C ₁₈ C ₁₆ C ₁₄ N ₁₁ (10)+ Γ C ₁₄ C ₁₆ C ₁₈ C ₁₇ (14)
8	222	214			2.13	3.70	5.07	0.15	β C ₁₈ C ₁₆ C ₁₄ (31)+ β C ₁₄ N ₁₁ N ₁₂ (12)+ β C ₉ C ₄ S ₅ (13)
9	255	245			2.44	3.70	4.10	0.16	β C ₁₈ C ₁₆ C ₁₄ (18)+ τ C ₃ C ₄ C ₉ N ₁₂ (14)+ τ C ₁₄ N ₁₁ N ₁₂ C ₉ (12)+ τ C ₁₆ C ₁₄ N ₁₁ N ₁₂ (20)
10	277	266			0.73	2.09	7.51	0.34	ν C ₂ C ₃ (11)+ ν N ₁₁ C ₁₄ (10)+ β N ₁₁ N ₁₂ C ₉ (28)
11	335	322			0.15	1.57	5.22	0.35	Γ C ₁ C ₂ S ₃ C ₃ (23)+ τ N ₁₁ N ₁₂ C ₉ C ₄ (36)+ τ C ₂ C ₃ C ₄ C ₉ (20)
12	358	344			0.78	2.34	8.73	0.66	ν C ₁₆ C ₁₄ (23)+ β N ₁₁ C ₁₄ O ₁₅ (20)+ β C ₂₁ N ₂₅ C ₁₉ (12)+ β C ₉ C ₄ S ₅ (12)
13	387	372			0.00	0.46	2.60	0.23	τ H ₂₀ C ₁₇ C ₁₉ N ₂₅ (20)+ τ C ₁₈ C ₁₉ C ₂₁ N ₂₅ (63)+ Γ C ₂₁ C ₁₈ N ₂₅ C ₁₆ (10)
14	413	397			1.99	1.22	6.36	0.64	β C ₁₆ C ₁₄ N ₁₁ (12)+ Γ N ₂₅ C ₁₉ C ₂₁ C ₁₈ (21)
15	488	469	468(vw)		2.27	0.79	5.33	0.75	Γ N ₂₅ C ₁₉ C ₂₁ C ₁₈ (19)+ Γ C ₁₄ C ₁₆ C ₁₈ C ₁₇ (13)
16	511	491	506(w)		0.70	0.22	4.77	0.73	Γ C ₁ C ₂ S ₃ C ₃ (57)+ τ C ₃ C ₂ C ₄ S ₅ (13)+ τ H ₁₃ N ₁₁ N ₁₂ C ₉ (15)
17	575	553			10.06	0.82	6.08	1.18	β N ₁₁ C ₁₄ O ₁₅ (27)+ β C ₂ C ₃ S ₅ (10)
18	583	560			0.36	0.53	3.19	0.64	Γ C ₁ C ₂ S ₃ C ₃ (15)+ τ C ₃ C ₄ S ₅ C ₂ (69)
19	602	578			7.39	9.88	1.56	0.33	τ H ₁₃ N ₁₁ N ₁₂ C ₉ (65)
20	634	609			0.77	9.01	3.51	0.83	ν S ₅ C ₄ (16)+ β C ₂ C ₃ S ₅ (12)+ β C ₁₆ C ₁₄ N ₁₁ (13)+ τ H ₁₃ N ₁₁ N ₁₂ C ₉ (17)
21	680	654		652(w)	0.43	1.78	6.90	1.88	β C ₁₇ C ₁₉ N ₂₅ (33)+ β C ₁₈ C ₂₁ N ₂₅ (30)
22	688	661			2.46	3.97	7.38	2.06	ν S ₅ C ₄ (12)+ β N ₁₁ C ₁₄ O ₁₅ (11)+ β N ₁₂ C ₉ C ₄ (25)+ β C ₂ C ₃ S ₅ (25)+ β C ₂₁ N ₂₅ C ₁₉ (14)
23	707	679	681(s)		3.53	0.80	4.94	1.45	ν S ₅ C ₄ (40)+ β C ₂ C ₃ C ₄ (10)
24	713	685			12.98	0.24	1.17	0.35	τ H ₆ C ₁ C ₂ C ₃ (70)+ Γ C ₂ C ₃ C ₄ H ₇ (24)
25	723	695			6.68	1.81	4.95	1.52	Γ C ₂₁ C ₁₈ N ₂₅ C ₁₆ (12)+ Γ O ₁₅ C ₁₆ N ₁₁ C ₁₄ (40)
26	748	719			1.39	1.50	6.87	2.26	ν S ₅ C ₁ (33)+ β C ₄ C ₃ C ₂ (25)
27	765	735	749(s)		3.61	0.57	2.58	0.89	τ H ₂₀ C ₁₇ C ₁₉ N ₂₅ (20)+ Γ C ₂₁ C ₁₈ N ₂₅ C ₁₆ (41)+ Γ N ₂₅ C ₁₉ C ₂₁ C ₁₈ (15)+ Γ O ₁₅ C ₁₆ N ₁₁ C ₁₄ (13)
28	802	771			3.45	1.12	4.64	1.76	ν C ₁₆ C ₁₄ (12)+ ν S ₅ C ₁ (11)+ β C ₁₈ C ₁₆ C ₁₄ (10)+ β N ₁₁ N ₁₂ C ₉ (16)
29	832	800			1.29	0.11	1.32	0.54	τ H ₆ C ₁ C ₂ C ₃ (17)+ Γ C ₃ C ₄ C ₉ H ₈ (68)
30	858	824			3.97	0.93	1.88	0.81	τ H ₂ C ₃ C ₄ C ₉ C ₁₇ C ₁₆ (56)+ Γ O ₁₅ C ₁₆ N ₁₁ C ₁₄ (11)+ Γ C ₁₄ C ₁₆ C ₁₈ C ₁₇ (13)
31	869	835			1.12	3.38	4.41	1.96	ν S ₅ C ₁ (22)+ β C ₂ C ₃ S ₅ (37)+ β C ₄ C ₃ C ₂ (21)
32	891	856	847(m)		0.42	0.27	1.26	0.59	τ H ₂₀ C ₁₇ C ₁₉ N ₂₅ (87)
33	916	881			0.01	0.30	1.32	0.65	τ H ₆ C ₁ C ₂ C ₃ (11)+ Γ C ₂ C ₃ C ₄ H ₇ (63)+ Γ C ₃ C ₂ C ₄ H ₈ (18)
34	947	909	903(m)	909(w)	2.08	1.52	1.51	0.80	τ H ₁₀ C ₉ N ₁₂ N ₁₁ (87)
35	984	946	935(w)		0.17	0.04	1.34	0.76	τ H ₂₀ C ₁₇ C ₁₉ N ₂₅ (67)+ Γ N ₂₅ C ₁₉ C ₂₁ C ₁₈ (12)
36	1002	963			0.29	0.20	1.51	0.89	τ H ₂₄ C ₂₁ N ₂₅ C ₁₉ (70)+ τ C ₁₈ C ₁₉ C ₂₁ N ₂₅ (13)
37	1012	973			0.65	8.17	6.37	3.84	ν N ₂₅ C ₁₉ (38)+ β C ₁₇ C ₁₉ N ₂₅ (16)+ β C ₁₈ C ₂₁ N ₂₅ (15)+ β C ₂₁ N ₂₅ C ₁₉ (14)
38	1068	1026			2.80	5.29	1.57	1.06	ν C ₃ C ₂ (44)+ β H ₈ C ₃ C ₂ (41)
39	1093	1050	1039(m)		2.61	1.01	2.11	1.49	ν C ₁₆ C ₁₈ (11)+ β H ₂₀ C ₁₇ C ₁₉ (20)+ β C ₁₇ C ₁₉ N ₂₅ (19)+ β C ₁₈ C ₂₁ N ₂₅ (23)
40	1106	1063		1061(m)	0.23	2.51	1.17	0.84	β H ₆ C ₁ S ₅ (46)+ β H ₈ C ₃ C ₂ (17)+ β H ₇ C ₂ C ₁ (11)
41	1111	1068			0.07	0.17	1.55	1.12	ν C ₁₆ C ₁₈ (39)+ β H ₂₀ C ₁₇ C ₁₉ (35)+ β H ₁₀ C ₉ N ₁₂ (10)
42	1130	1086		1082(w)	0.65	27.34	3.84	2.89	ν C ₁₆ C ₁₈ (25)+ ν N ₁₁ N ₁₂ (17)+ β H ₂₀ C ₁₇ C ₁₉ (10)
43	1174	1128			28.52	39.50	3.61	2.93	ν N ₁₁ C ₁₄ (12)+ ν N ₁₁ N ₁₂ (46)
44	1244	1195			1.50	2.79	1.33	1.21	ν N ₂₅ C ₁₉ (24)+ β H ₂₀ C ₁₇ C ₁₉ (25)+ β H ₂₄ C ₂₁ C ₁₈ (33)
45	1247	1198			6.57	4.79	1.51	1.39	ν C ₄ C ₉ (13)+ β H ₈ C ₃ C ₂ (50)
46	1253	1203			0.50	14.66	4.24	3.92	ν C ₂ C ₃ (34)+ β C ₄ C ₃ C ₂ (13)
47	1275	1225	1217(m)	1222(m)	0.84	0.83	11.92	11.41	ν N ₂₅ C ₁₉ (52)+ ν C ₁₈ C ₂₁ (10)+ ν C ₁₆ C ₁₇ (27)
48	1329	1277			49.48	4.21	1.89	1.96	ν N ₁₁ C ₁₄ (17)+ ν C ₁₆ C ₁₄ (10)+ β H ₁₀ C ₉ C ₄ (33)
49	1353	1300	1291(m)	1299(s)	0.99	0.62	1.41	1.52	ν C ₁₈ C ₂₁ (11)+ β H ₂₀ C ₁₇ C ₁₉ (40)+ β H ₂₃ C ₁₉ N ₂₅ (15)
50	1366	1312		1321(m)	56.82	14.80	2.48	2.72	ν N ₁₁ C ₁₄ (17)+ ν C ₁₆ C ₁₄ (10)
51	1390	1335			2.92	0.86	1.91	2.17	ν C ₃ C ₂ (11)+ β H ₁₃ N ₁₁ N ₁₂ (10)+ β H ₆ C ₁ S ₅ (15)+ β H ₇ C ₂ C ₁ (18)+ β H ₁₀ C ₉ C ₄ (15)
52	1438	1382	1363(w)	1367(w)	4.78	0.42	1.91	2.33	ν C ₁₈ C ₂₁ (27)+ β H ₂₃ C ₁₉ N ₂₅ (50)
53	1461	1404	1415(m)		3.51	106.30	4.04	5.09	ν C ₄ C ₃ (40)+ ν C ₃ C ₂ (19)+ β H ₁₃ N ₁₁ N ₁₂ (11)+ β H ₇ C ₂ C ₁ (11)
54	1508	1449			12.04	3.21	2.19	2.93	ν C ₂ C ₁ (19)+ β H ₁₃ N ₁₁ N ₁₂ (40)
55	1521	1462			2.24	2.55	2.18	2.97	ν N ₂₅ C ₂₁ (19)+ ν C ₁₆ C ₁₈ (12)+ β H ₂₀ C ₁₇ C ₁₉ (20)+ β H ₂₄ C ₂₁ C ₁₈ (36)
56	1569	1507		1513(w)	4.54	3.06	4.75	6.88	ν C ₂ C ₁ (55)+ β H ₇ C ₂ C ₁ (14)
57	1593	1531			5.26	0.68	7.58	11.35	ν N ₂₅ C ₁₉ (30)+ ν C ₁₆ C ₁₇ (46)
58	1631	1568	1574(s)		1.52	6.67	5.39	8.45	ν C ₁₆ C ₁₈ (66)+ β H ₂₀ C ₁₇ C ₁₉ (11)
59	1660	1594	1595(s)		0.62	236.38	7.82	12.68	ν N ₁₂ C ₉ (71)+ β H ₁₀ C ₉ C ₄ (11)
60	1728	1660	1666(s)	1664(m)	100.00	17.77	7.80	13.73	ν O ₁₅ C ₁₄ (78)
61	3036	2917			6.92	2.27	1.09	5.90	ν C ₉ H ₁₀ (100)
62	3153	3029	3027(m)		4.80	1.93	1.09	6.37	ν C ₁₉ H ₂₃ (71)+ ν C ₂₁ H ₂₄ (28)
63	3156	3033			1.56	3.22	1.09	6.41	ν C ₁₉ H ₂₃ (28)+ ν C ₂₁ H ₂₄ (69)
64	3196	3070		3067(w)	0.89	1.94	1.09	6.56	ν C ₂ H ₇ (21)+ ν C ₃ H ₈ (79)
65	3204	3079			0.55	2.10	1.09	6.61	ν C ₁₈ H ₂₂ (97)
66	3212	3086			0.90	3.94	1.09	6.65	ν C ₂ H ₇ (72)+ ν C ₃ H ₈ (21)
67	3226	3099		3090(w)	0.33	1.61	1.09	6.70	ν C ₁₇ H ₂₀ (98)
68	3243	3116			0.10	3.72	1.10	6.80	ν C ₁ H ₆ (92)
69	3469	3333			1.39	4.49	1.08	7.62	ν N ₁₁ H ₁₃ (100)

ν : Stretching, β : in-plane-bending, Γ : out-of-plane bending, τ : Torsion, vw: very weak, w: weak, m: medium, s: strong, vs: very strong, ^aScaling factor: 0.9608, ^bRelative IR absorption intensities normalized with highest peak absorption equal to 100, ^cRelative Raman intensities and normalized to 100., ^dTotal energy distribution calculated at B3LYP/6-311++G(d,p) level.

3.3. UV-Visible spectral analysis

The analysis of the wave function indicates that the electron absorption corresponds to the transition from the ground to the first excited state and is mainly described by one-electron excitation from the HOMO to LUMO, HOMO-1 to LUMO+1 and HOMO-2 to LUMO+2 levels, etc. The calculated absorption wavelengths (λ), oscillator strengths (f) and excitation energies (E) are presented in Table 3. It is noted from the Table 3, that the calculated absorption maxing values are: 323, 298 and 281 nm, which correlated well with the experimental values 345, 305 nm. The major contributions of the transitions were assigned with the aid of SWizard program (Gorelsky, 2013). In view of calculated absorption spectra, the maximum absorption wavelength $\lambda_{(max)}$ = 345 nm corresponds to the electronic transition from the HOMO to LUMO+1 (82%) contribution. The calculated absorption maxima value is assigned as π - π^* transition, which is attributed to the presence of large no of free lone pairs of electrons available on sulphur (S₅), Nitrogen (N₁₁, N₁₂) and Oxygen (O₁₅) atoms. The observed and calculated UV-Visible spectra are shown in Fig. 4. The calculated/experimental wavelengths, excitation energies, oscillator strength and type of transition are listed in Table 5. The absorption maxima (λ_{max} = 345 nm) is red shifted on comparing with literature (Bharanidharan et al., 2017), which may be due to charge separation of carbonyl group molecule in solution state.

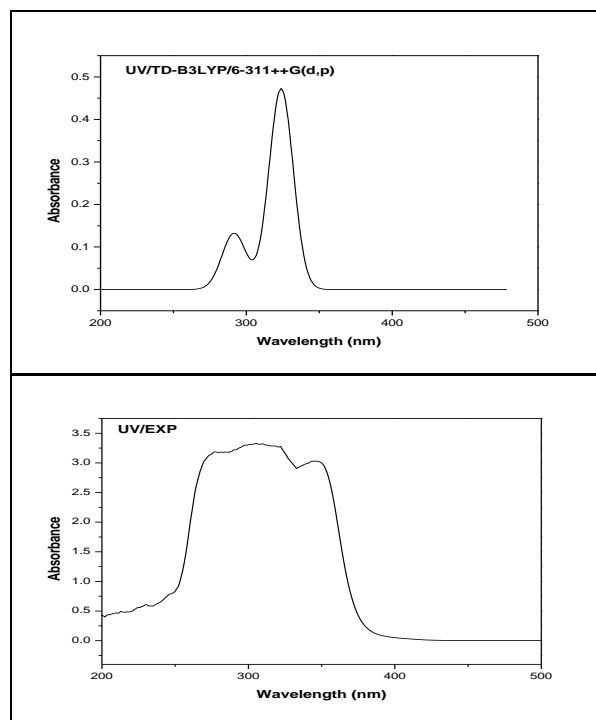


Fig. 4: The Combined Theoretical and Experimental UV-Visible Spectra of TMINH.

Table 3: The Electronic Transition of TMINH

Calculated at B3LYP/6-311++G(d,p)	Oscillator strength	Calculated Band gap (eV/nm)	Experimental Band gap (nm)	Type
Excited State1	Singlet-A (f=0.4727)	3.8286 eV/323.83 nm	345	
60 -> 61	0.61280	4.0054		
60 -> 62	-0.21671	3.0954		
Excited State2	Singlet-A (f=0.0104)	4.1492eV/298.81 nm	305	π - π^*
59 -> 61	0.55858	4.132035		
59 -> 62	-0.38574	3.259369		
Excited State3	Singlet-A (f=0.0193)	4.3995 eV/281.81 nm		
69 -> 76	0.10311	4.132035		
70 -> 76	0.21172	3.678423		

3.4. NMR analysis

The experimental ^1H and ^{13}C NMR chemical shifts values are compared with the theoretical data. The chemical shift for ^1H atoms of TMINH are fall in the range of 8.55-6.04 ppm. Some chemical shifts are deshielded since the hydrogen atoms are bonded or nearby with the electronegative atoms. Hydrogen attached with nearby electron-donating atom or group increases the shielding and moves the resonance towards to a lower frequency, whereas electron-withdrawing atom or group can decrease the shielding and move the resonance of attached proton towards to a higher frequency region (Chamberlain, 1974). The downfield signal at 6.98 ppm is assigned to azomethine hydrogen H₁₀. The aromatic protons appear in the range 6.10 to 7.50 ppm. The upfield signal at 5.83 ppm is assigned to N-H (H₁₃) proton. In ^{13}C NMR spectrum of TMINH revealed that the signal appeared at 199.51 ppm is due to C=O carbon and the signal appeared at 158.86 ppm is responsible for C=N carbon atom. The C₁₄ carbon resonance occurs at downfield region when compare to C₉ carbon is due to the presence of higher electronegative oxygen atom. The experimental and calculated values for ^{13}C and ^1H NMR are shown in Table 4. The observed ^1H and ^{13}C NMR spectra of TMINH is plotted in Figs. 5a -5b.

Table 4: Experimental and Calculated ^1H and ^{13}C Chemical Shift (Ppm) Values TMINH

Atoms (TMINH)	Theoretical	Experimental
H23	8.55	7.50
H24	8.49	7.49
H10	8.38	6.98
H20	8.28	7.45
H6	8.21	7.44
H22	8.19	6.98
H8	7.95	6.49
H7	6.65	5.98
H13	6.04	5.83
C14	208.04	199.51
C9	168.66	158.86
C19	156.38	147.02
C21	155.34	147.02
C4	154.67	141.28
C3	149.11	141.28
C16	144.15	137.55
C2	143.82	137.55
C1	131.16	124.35
C17	128.05	124.35
C18	121.72	118.42

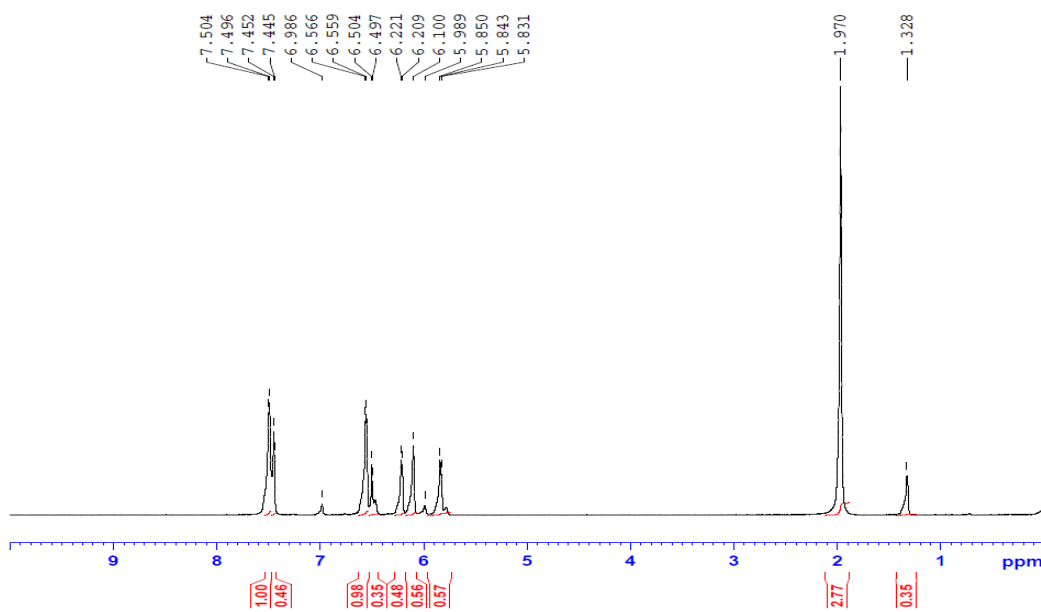


Fig. 5: A) ^1H NMR Spectrum of Compound TMINH

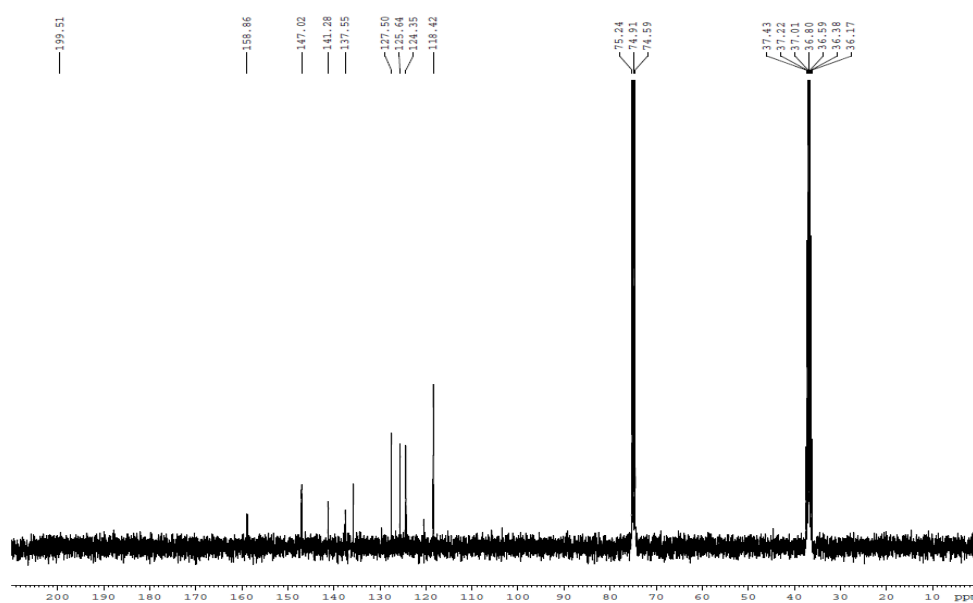


Fig. 5: B) ^{13}C NMR Spectrum of Compound TMINH.

Table 5: The NLO Measurements of TMINH

Parameters	B3LYP/6-311++G(d,p)
Dipole moment (μ) Debye	
μ_x	0.3145
μ_y	-0.7701
μ_z	0.5380
M	0.9906 Debye
Hyperpolarizability (β_0) $\times 10^{-30}$ esu	
β_{xxx}	-1853.85
β_{xxv}	229.60
β_{xyy}	-33.45
β_{yyy}	-129.96
β_{xxz}	40.31
β_{xyz}	21.11
β_{vzv}	2.92
β_{xzz}	54.46
β_{vzz}	-29.90
β_{zzz}	-38.55
β_0	1.5861 $\times 10^{-30}$ esu

Standard value for urea ($\mu=1.3732$ Debye, $\beta_0=0.3728 \times 10^{-30}$ esu): esu-electrostatic unit.

3.5. Polarizability and hyper polarizability

The NLO activity provide the key functions for frequency shifting, optical modulation, optical switching and optical logical for the developing technologies in areas such as communication, signal processing and optical inter-connections (Andraud et al., 1994;

Geskin et al., 2003). NLO describes the behavior of media, in which the dielectric polarizability 'P' responds non-linearly to the electric field E of the light. In this study, the polarizability ($\alpha_0=0.5318 \times 10^{-30}$ esu), first order hyperpolarizability ($\beta_0=1.5861 \times 10^{-30}$ esu) and total dipole moment ($\mu=0.9906$ Debye) are calculated and listed in Table 5. The first order hyperpolarizability β_0 value is four times greater than that of urea. On comparing with T2CNH (Bharanidharan et al., 2017) β_0 value is 1.5 time greater than that of T2CNH. This is due to the fact that the para position of pyridine.

3.6. Natural bond orbital analysis

NBO analysis is an essential tool for studying intra- and inter-molecular bonding interactions, and also a convenient basis for investigating charge transfer or conjugative interaction in molecular systems. Some orbitals are electron donor and some are acceptors, the energy difference between such bonding and anti-bonding orbitals makes the molecule susceptible for interactions (Liu et al., 2005; James et al., 2006). The larger energy difference $E^{(2)}$ value, the more intensive is the interaction i.e. more is donating tendency of electron from one orbital and more is the accepting tendency of other orbital, which makes the interaction between them stronger. The analysis of the various donors and acceptors indicate that there are only two types of donors σ & π , and two types of acceptors σ^* & π^* , respectively.

The various acceptors for different donor clearly indicate that the intra-molecular interaction are found by the orbital overlap between different bonding and respective anti-bonding orbitals, which results intra-molecular charge transfer (ICT) causing stabilization of the system (Liu et al., 2005). These interactions increase with increase in electron density (ED) difference and the stabilization energy $E^{(2)}$ between the donor and acceptor levels of C-C, C-H bonding and anti-bonding orbitals. The $E^{(2)}$ energy values and types of the transition are shown in Table 6. The strong intra-molecular hyperconjugative interaction of the σ and π electrons of C-C, C=C, C=N to the anti C-C, C=C, C=N bonds of the ring as well as C=O group leads to stabilization of some part of the ring system in TMINH. The hyperconjugative interactions $\pi(C_1-C_2) \rightarrow \pi^*(C_3-C_4)$, $\pi(C_3-C_4) \rightarrow \pi^*(C_9-N_{12})$, $\pi(C_{16}-C_{17}) \rightarrow \pi^*(C_{19}-N_{25})$, $\pi(C_{18}-C_{21}) \rightarrow \pi^*(C_{16}-C_{17})$ & $\pi(C_{19}-N_{25}) \rightarrow \pi^*(C_{18}-C_{21})$ transfer more stabilization energy: 66.15, 86.90, 109.45, 91.71 & 104.47 kJ/mol to the molecular system. In TMINH, the lone pair of sulphur, nitrogen and oxygen atoms play great role, i.e. the S₅, N₁₁ & O₁₅ atoms transfer maximum energy 95.14, 188.82 & 104.18 kJ/mol to (C₁-C₂), (C₁₄-O₁₅) & (N₁₁-C₁₄) bonds, respectively. In hetero atoms, the maximum hyperconjugative $E^{(2)}$ energy exhibited during the inter-molecular interaction, which leads the molecule towards medicinal and biological application (Liu et al., 2005). The $\nu(C_1-S_5)$ mode observe at higher frequency (719 cm^{-1} /mode no: 26) than the $\nu(C_4-S_5)$ mode (679 cm^{-1} /mode no: 23), since the bond $\sigma(C_3-H_8)$ transfer more energy (22.72 kJ/mol) to $\sigma^*(C_4-S_5)$ bond on comparing with energy transfer (18.7 kJ/mol) from $\sigma(C_2-H_7)$ to $\sigma^*(C_1-S_5)$ bond.

3.7. HOMO-LUMO analysis

The ionization potential is determined from the energy difference between the energy of the compound derived from electron-transfer (radical cation) and the respective neutral compound; $IP = E_{cation} - E_n$; $IP = -E_{HOMO}$, while the electron affinity is computed from the energy difference between the neutral molecule and the anion molecule: $EA = E_n - E_{anion}$; $EA = -E_{LUMO}$, respectively. The other important quantities such as electro negativity (χ), hardness (η), softness (ζ), and Electrophilicity index (ω) are deduced from ionization potential and electron affinity values (Kohn et al., 1996;

Parr and Pearson, 1983; Politzer and Abu-Awwad, 1998) using the following equations:

$$\text{Electro negativity } (\chi) \mu \approx -\chi = -\frac{IP+EA}{2}$$

$$\text{Chemical hardness } (\eta) \approx \frac{IP-EA}{2}$$

$$\text{Softness } (\zeta) = \frac{1}{\eta}$$

$$\text{And Electrophilicity index } (\omega) = \frac{x^2}{2\eta}$$

The energy values of HOMO, LUMO, energy gap, electron affinity, electrophilicity index, chemical hardness and softness of the title molecule are listed in Table 7. For the present molecule, the HOMO, LUMO and band gap energies are calculated in gas phase: -6.4074 eV, -2.2829 eV, and 4.1245 eV, respectively. These observations are less on comparing with T2CNH (Bharanidharan et al., 2017), which leads the molecule TMINH becomes less stable and more reactive. The HOMO is located over entire molecule except pyridine ring and LUMO is located over entire molecule. The HOMO-LUMO picture is shown in Fig. 6.

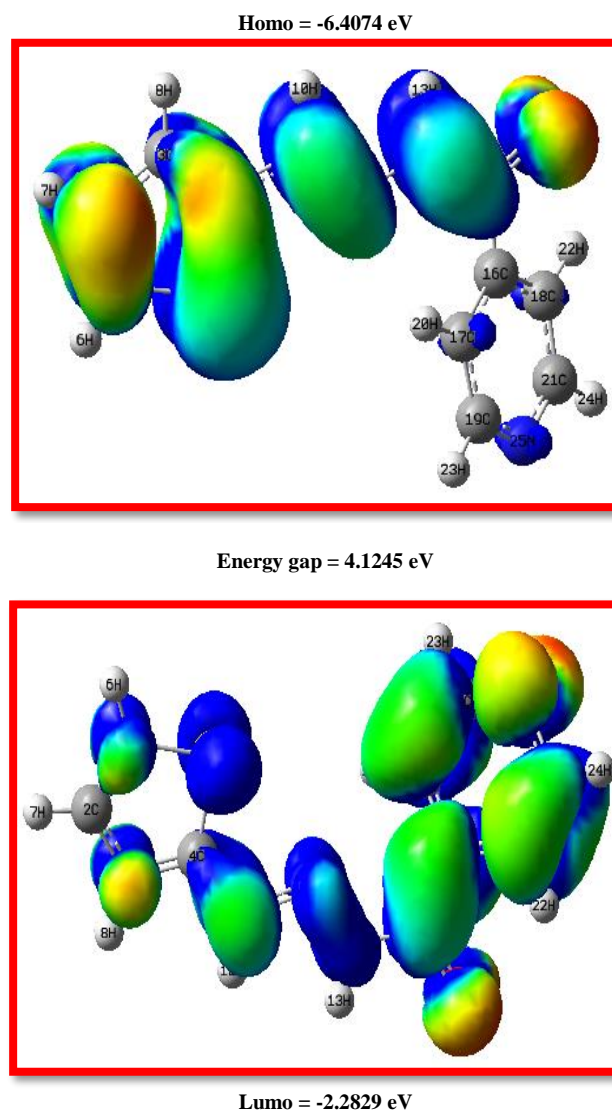


Fig. 6: The Frontier Molecular Orbitals of TMINH.

Table 6: The Second Order Perturbation Theory Analysis of Fock Matrix in NBO Basis for TMINH

Type	Donor NBO (i)	ED/e	Acceptor NBO (j)	ED/e	^a E ⁽²⁾ KJ/mol	^b E(j)-E(i) a.u.	^c F(i,j) a.u.
π - π^*	BD (2) C1 - C2	1.84953	BD*(2) C3 - C4	0.36084	66.15	0.29	0.064
σ - σ^*	BD (1) C2 - H7	1.97661	BD*(1) C1 - C2	0.01456	6.15	1.13	0.036
			BD*(1) C1 - S5	0.01837	18.7	0.76	0.052
			BD*(1) C3 - C4	0.01786	7.95	1.12	0.041
π - π^*	BD (2) C3 - C4	1.79964	BD*(2) C1 - C2	0.29744	65.19	0.29	0.061
			BD*(2) C9 - N12	0.22717	86.90	0.28	0.068
σ - σ^*	BD (1) C3 - H8	1.97446	BD*(1) C1 - C2	0.01456	7.61	1.13	0.041
			BD*(1) C3 - C4	0.01786	6.9	1.12	0.038
			BD*(1) C4 - S5	0.03599	22.72	0.75	0.057
π - π^*	BD (2) C16 - C17	1.6346	BD*(2) C14 - O15	0.27322	63.01	0.29	0.06
			BD*(2) C18 - C21	0.28244	75.48	0.29	0.066
			BD*(2) C19 - N25	0.36974	109.45	0.27	0.075
π - π^*	BD (2) C18 - C21	1.61935	BD*(2) C16 - C17	0.34396	91.71	0.28	0.071
			BD*(2) C19 - N25	0.36974	77.91	0.27	0.063
π - π^*	BD (2) C19 - N25	1.70768	BD*(2) C16 - C17	0.34396	60.12	0.32	0.061
			BD*(2) C18 - C21	0.28244	104.47	0.32	0.08
n- σ^*	LP (1) S5	1.98423	BD*(1) C1 - C2	0.01456	8.24	1.24	0.044
			BD*(1) C3 - C4	0.01786	10.29	1.23	0.049
n- π^*	LP (2) S5	1.61766	BD*(2) C1 - C2	0.29744	95.14	0.26	0.07
			BD*(2) C3 - C4	0.36084	93.72	0.26	0.068
n- π^*	LP (1) N11	1.6583	BD*(2) C9 - N12	0.22717	120.42	0.28	0.083
			BD*(1) C14 - O15	0.01761	4.23	0.86	0.029
			BD*(2) C14 - O15	0.27322	188.82	0.31	0.108
n- σ^*	LP (1) O15	1.97996	BD*(1) C14 - C16	0.06793	8.54	1.11	0.043
n- σ^*	LP (2) O15	1.86488	BD*(1) N11 - C14	0.07478	104.18	0.68	0.118
			BD*(1) C14 - C16	0.06793	75.86	0.67	0.1
n- σ^*	LP (1) N25	1.91907	BD*(1) C17 - C19	0.02611	38.66	0.9	0.083
			BD*(1) C18 - C21	0.02457	37.66	0.91	0.082
			BD*(1) C19 - H23	0.02383	17.07	0.77	0.051
			BD*(1) C21 - H24	0.02374	16.82	0.77	0.05

^a E⁽²⁾ means energy of hyper conjugative interaction (stabilization energy).

^b Energy difference between donor (i) and acceptor(j) nbo orbitals.

^c F(i,j) is the Fock matrix element between i and j nbo orbitals.

Table 7: The Physico-Chemical Properties of TMINH

Parameters	Values
HOMO	-6.4074 eV
LUMO	-2.2829 eV
Energy gap	4.1245 eV
Ionization potential (IP)	6.4074 eV
Electron affinity (EA)	2.2829 eV
Electrophilicity Index (ω)	2.2887
Chemical Potential (μ)	4.3451
Electro negativity (χ)	-4.3451 eV
Hardness (η)	-4.1245

3.8. Molecular electrostatic potential

In the present study, a 3D MEP plot of TMINH molecule is shown in Fig. 7. The plot of electrostatic potential is based on the ED distribution within the molecule at different points. The red color in the map indicates the negatively charged region and the blue colour indicate the positive region, while the green colour indicates the neutral region. The oxygen atom (O₁₅) in the C=O group and hydrogen atoms in hydrazone linkage covered respectively by Red and blue region, while the rest of the molecule is neutral. The positive and negative potential of the molecule ranges from $-7.560 e^{-2}$ a.u. to $7.560 e^{-2}$ a.u. These two ends of the molecule which are positively and negatively charged are prone to electrophilic and nucleophilic attack of the title molecule.

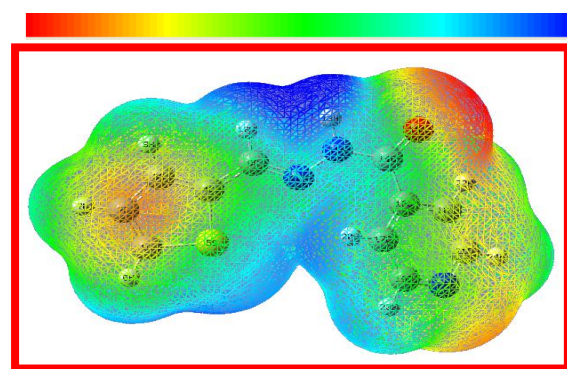


Fig. 7: The Molecular Electrostatic Potential Map of TMINH.

3.9. Mulliken atomic charges

The calculation of atomic charges plays an important role in the application of quantum mechanical calculations to molecular systems (Gunasekaran et al., 2008). The calculated mulliken atomic charges are listed in Table 8 and plotted in Fig. 8 shows

that the C₂/C₃ atoms have highest negative/positive charges, respectively among the other atoms in TMINH due to the resonance. The H₆& H₁₃ atoms have the largest positive charges among the other hydrogen atoms. Similarly, N₁₁/N₁₂ atoms have more negative/positive charges on comparing with N₂₅ atom. This may be due to not only N₂₅ atom and also due to O₁₅ atom having more electronegativity than nitrogen.

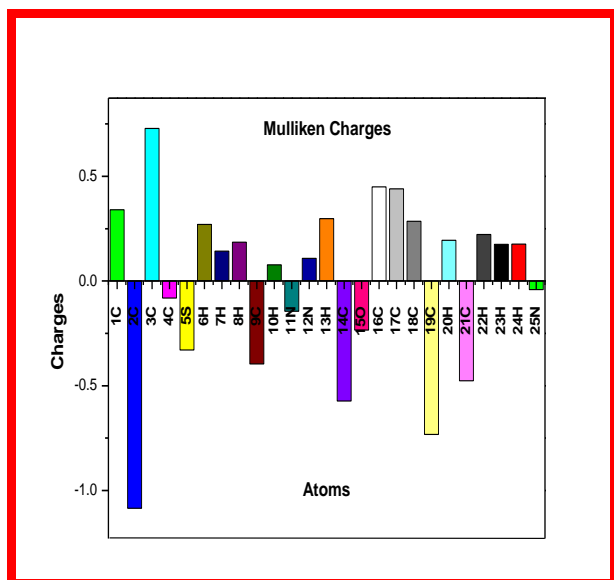


Fig. 8: The Mulliken Atomic Charges of TMINH

Table 8: The Mulliken Atomic Charges of TMINH

Atoms	Charges	Atoms	Charges
1C	0.33983	14C	-0.572448
2C	-1.084829	15O	-0.234077
3C	0.728187	16C	0.44918
4C	-0.080825	17C	0.440253
5S	-0.329715	18C	0.284785
6H	0.270504	19C	-0.732119
7H	0.142876	20H	0.194408
8H	0.184643	21C	-0.476341
9C	-0.395881	22H	0.22227
10H	0.076824	23H	0.175399
11N	-0.144584	24H	0.176213
12N	0.107845	25N	-0.040634
13H	0.298237		

Table 9: Thermodynamic Parameters of TMINH at Different Temperatures

T (K)	S (J/mol.K)	C _p (J/mol.K)	ΔH (kJ/mol)
100.00	346.85	98.21	6.85
200.00	432.57	157.89	19.56
298.15	507.83	223.62	38.27
300.00	509.22	224.85	38.69
400.00	582.63	286.94	64.36
500.00	652.40	338.36	95.72
600.00	717.85	379.26	131.68
700.00	778.84	411.77	171.29
800.00	835.60	438.00	213.82
900.00	888.47	459.52	258.73
1000.00	937.84	477.43	305.60

3.10. Thermodynamic properties

On the basis of vibrational analysis carried out at B3LYP/6-311++G(d,p) level, the standard statistical thermodynamic functions such as: heat capacity (C_p), entropy (S) and enthalpy changes (ΔH) are calculated for the present molecule and the values are listed in Table 9. It can be observed that these thermodynamic functions are increasing with temperature. The obvious reason for this almost linear increase is due to the increase in internal energy of the molecule in accordance with the kinetic theory of gases (BevenOtt and Boerio-Goates, 2000). The correlation equations between thermodynamic functions and temperatures were fitted by quadratic formula and the corresponding fitting factors (R²) for these thermodynamic properties are found to be 0.99876, 0.99942 and 0.99998, respectively. The corresponding correlation graphs are shown in Fig. 9.

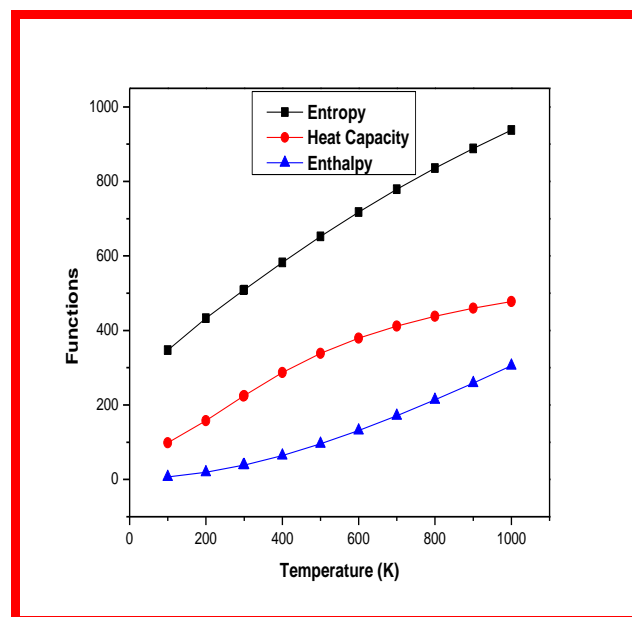


Fig. 9: The Thermodynamic Properties of TMINH at Different Temperatures.

3.11. Molecular docking studies

Molecular docking studies were carried out to study the precise binding site of ligand on protein. A molecular docking study is a key tool in structural molecular biology and computer-assisted drug design. The synthesized analogue docked with crystal structure of human lanosterol 14- α dimethylase in complex with ketaconazole (3LD6). Analogue showed best ligand pose energy -6.7 kcal/mol in 3LD6 protein. The protein ligand interactions are shown in Fig. 10. The ligand is surrounded by hydrophobic interactions of amino acids like PHE152, PHE139, MET304, ALA144, LEU308, VAL143, LEU159, TYR131, ALA311, PHE234, MET380, and ILE377. The blue color indicates THR135 polar the HEM601 unspecified residue and the GLY307 water. The TYR145, hydrozone linkage in hydrozone bond interaction and the bond distance is 2.05 Å. From this interaction it can be predicted as the activity may be due to inhibition of human lanosterol 14- α dimethylase in complex with ketaconazole.

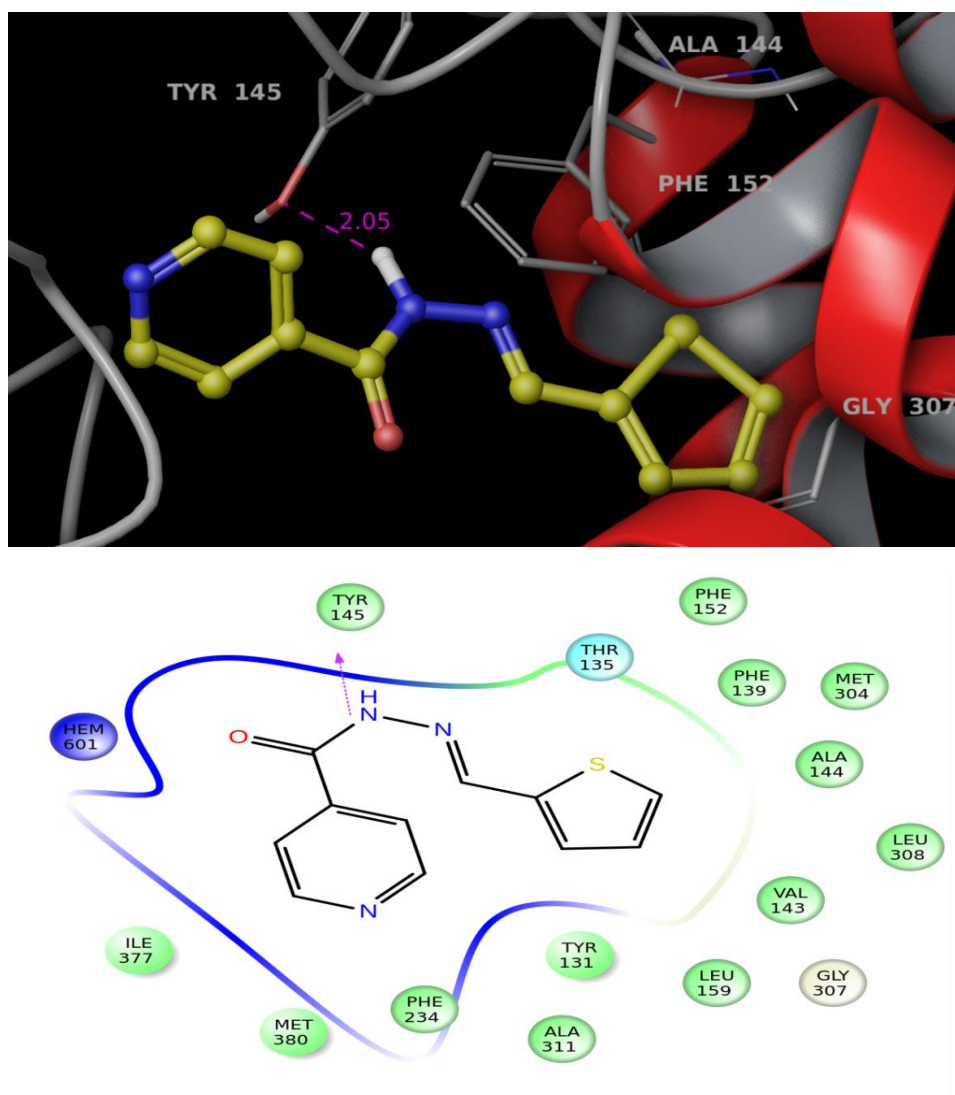


Fig. 10:2D And 3D Interaction of Compound TMINH.

4. Conclusion

The FT-IR, FT-Raman and UV-Vis spectra of the Schiff base compound TMINH had been recorded and analyzed for first time. The detailed interpretations of the vibrational spectra have been carried out. The optimized geometrical parameters were calculated and compared with the reported XRD data. In TMINH, the thiophene and hydrazone moieties were co-planar. On the basis of the agreement between the calculated and experimental results, assignments of all the fundamental vibrational modes of TMINH are examined and proposed in this investigation. The NBO result reflects more hyperconjugative interaction energy during π -electron transfer within π - π^* interaction and it leads that the molecule become more active. The lowering of the HOMO-LUMO energy gap value has substantial influence on the ICT and bioactivity of the molecule. The lowering /increasing of wavenumbers may be due to delocalization of electronic cloud present in the pyridine ring. The TD-DFT calculation of the UV spectrum shows moderate agreement with experimental observations. Besides the first hyperpolarizability value of the molecule is found to be high i.e. six times greater than that of urea, hence the NLO activity of the molecule will also be proportionately high. The MEP surface predicts the nucleophilic and electrophilic reaction sites of the molecule. The thermodynamic properties such as heat capacity, entropy and enthalpy at different temperature were also calculated. The docking study clearly indicates that the test compound TMINH display hydrogen bonding interaction with tyrosine-145 amino

acid present in the active site with the magnitude of 2.05 Å. Due to the presence of electronegative oxygen atom, the C₁₄ carbon appears in the downfield region when compare to C₉ carbon.

References

- [1] Davidson, E.R., 2000, Computational Transition Metal Chemistry, Chemical Reviews, 100(2), 351–352. <https://doi.org/10.1021/cr980385s>.
- [2] Molvi, K.I., Vasu, K.K., Yerande, S.G., Sudarsanam, V., &Haque, N., 2007, Syntheses of new tetrasubstitutedthiophenes as novel anti-inflammatory agents, Eur. J. Med. Chem, 42(8), 1049–1058. <https://doi.org/10.1016/j.ejmech.2007.01.007>.
- [3] SatheeshaRai, N., Kalluraya, B., Lingappa, B., Shenoy, S., &Puranic, V.G., 2008, Convenient access to 1,3,4-trisubstituted pyrazoles carrying 5-nitrothiophene moiety via 1,3-dipolar cycloaddition of sydnone with acetylenic ketones and their antimicrobial evaluation, Eur. J. Med. Chem. 43(8), 1715–1720, <https://doi.org/10.1016/j.ejmech.2007.08.002>.
- [4] Ashalatha, B.V., Narayana, B., Vijaya Raj, K.K., & Suchetha Kumari, N., 2007, Synthesis of some new bioactive 3-amino-2-mercapto-5,6,7,8-tetrahydro[1]benzothieno[2,3-d]pyrimidin-4(3H)-one derivatives, Eur. J. Med. Chem. 42(5), 719–728. <https://doi.org/10.1016/j.ejmech.2006.11.007>.
- [5] Polívka, Z., Holubek, J., Svátek, E., Metyš, J., &Protiva, M., 1984, Potential hypnotics and anxiolytics: Synthesis of 2-bromo-4-(2-chlorophenyl)-9-[4-(2-methoxyethyl)piperazino]-6H-thieno [3,2,4-triazolo[4,3-a]-1,4-diazepine and of some related compounds, Collect. Czech. Chem. Commun. 49(3), 621–636. <https://doi.org/10.1135/cccc19840621>.
- [6] Noguchi, H., Kitazumi, K., Mori, M., &Shiba, T., 2004, Electroencephalographic Properties of Zaleplon, a Non-

- Benzodiazepine Sedative/Hypnotic, in Rats, J. Pharm. Sci. 94(3), 246–251. doi:10.1254/jphs.94.246. <https://doi.org/10.1254/jphs.94.246>.
- [7] Guentert, M., Bertram, H.-J., Emberger, R., Hopp, R., Sommer, H., & Werkhoff, P., 2010, ChemInform Abstract: Thermal Degradation of Thiamin (Vitamin B1). A Comprehensive Survey of the Latest Studies. ChemInform, 25(49), no-no. <https://doi.org/10.1002/chin.199449312>.
- [8] Press, J.B., 1991, the chemistry of heterocyclic compounds, thiophene and its derivatives, in: Gronowitz, S., (Ed.), 44(4), 397–502, John Wiley and Sons, New York.
- [9] Bloor, D., 1995, Good conduct: Now that researchers have overcome problems with synthesizing and manipulating conductive polymers, these materials are beginning to fulfil their early potential. Chemistry in Britain, 31(5), 385–385.
- [10] Nalwa, H.S., 1993, Organic Materials for Third-Order Nonlinear Optics, Advanced Materials, 5(5), 341–358. <https://doi.org/10.1002/adma.19930050504>.
- [11] Wu, I.Y., Lin, J.T., Li, C.S., Wang, W.C., Huang, T.H., Wen, Y.S., Tsai, C., 1999, Preparation of push-pull type chromophores via nitrothiophene induced Michael type reaction of alkynes, Tetrahedron, 55(49), 13973–13982. [https://doi.org/10.1016/S0040-4020\(99\)00871-6](https://doi.org/10.1016/S0040-4020(99)00871-6).
- [12] Mansour, A., Eid, M., & Khalil, N., 2003, Synthesis and Reactions of Some New Heterocyclic Carbohydrazides and Related Compounds as Potential Anticancer Agents. Molecules, 8(12), 744–755. <https://doi.org/10.3390/81000744>.
- [13] Metwally, K.A., Abdel-Aziz, L.M., Lashine, E.S. M., Husseiny, M.I., & Badawy, R.H., 2006, Hydrazones of 2-aryl-quinoline-4-carboxylic acid hydrazides: Synthesis and preliminary evaluation as antimicrobial agents. Bio. Org. & Med. Chem., 14(24), 8675–8682. <https://doi.org/10.1016/j.bmc.2006.08.022>.
- [14] Ghiglieri-Bertez, C., Coquelet, C., Alazet, A., & Bonne, C., 1987, Inhibiteurs mixtes des voies de la cyclooxygénase et des lipooxygénases: synthèse et activité de dérivés hydrazoniques, J. Med. Chem. 22(2), 147–152. [https://doi.org/10.1016/0223-5234\(87\)90010-9](https://doi.org/10.1016/0223-5234(87)90010-9).
- [15] Gaussian 03 Program, 2004, Gaussian Inc, Wallingford CT.
- [16] Frisch, A., Nielson, A.B., Holder, A.J., 2000, GAUSSVIEW User Manual Gaussian Inc. Pittsburgh, PA.
- [17] Jamroz, M.H., 2004, Vibrational Energy Distribution Analysis, VEDA 4 Computer Program, Poland.
- [18] Glendening, E.D., Reed, A.E., Carpenter, J.E., Weinhold, F., 1998, NBO Version 3.1, TCI, University of Wisconsin, Madison.
- [19] 3LD6 reference from PDB.
- [20] Protein Preparation Wizard; Epik Version 2.3, Impact version 5.7, Schrödinger, LLC, New York, 2014–4 release.
- [21] Jorgensen, W.L., Maxwell, D.S., & Tirado-Rives, J., 1996, Development and Testing of the OPLS All-Atom Force Field on Conformational Energetics and Properties of Organic Liquids, J. Am. Chem. Soc. 118(45), 11225–11236. <https://doi.org/10.1021/ja9621760>.
- [22] Glide Version 5.8, Schrödinger, LLC, New York, 2014–4 release.
- [23] Maestro, Schrödinger, LLC, New York, 2014–4 release.
- [24] Ligprep, Version 2.5, Schrödinger, LLC, New York, 2014–4 release.
- [25] Balachandran, V., Janaki, A., & Nataraj, A., 2014, Theoretical investigations on molecular structure, vibrational spectra, HOMO, LUMO, NBO analysis and hyperpolarizability calculations of thiophene-2-carbohydrazide, 118, 321–330. <https://doi.org/10.1016/j.saa.2013.08.091>.
- [26] Fleming, G. D., Koch, R., & Campos Vallete, M. M. (2006). Theoretical study of the syn and anti thiophene-2-aldehyde conformers using density functional theory and normal coordinate analysis, Spectrochim Acta A, 65(3-4), 935–945. <https://doi.org/10.1016/j.saa.2006.01.038>.
- [27] Song, M.Z., & Fan, C.G., 2009, (E)-N²-(2-Furylmethylene)benzohydrazide, Acta Crystallographica Sec. E Structure Reports, 65(11), o2800, <https://doi.org/10.1107/S1600536809042251>.
- [28] Rauhut, G., & Pulay, P., 1995, Transferable Scaling Factors for Density Functional Derived Vibrational Force Fields. J. Phys. Chem., 99(10), 3093–3100. <https://doi.org/10.1021/j100010a019>.
- [29] Nagabalasubramanian, P.B., Karabacak, M., & Periandy, S., 2012, Vibrational frequencies, structural confirmation stability and HOMO–LUMO analysis of nicotinic acid ethyl ester with experimental (FT-IR and FT-Raman) techniques and quantum mechanical calculations. J. Mol. Struct., 1017, 1–13. <https://doi.org/10.1016/j.molstruc.2012.02.042>.
- [30] Krishnakumar, V., Balachandran, V., & Chithambarathanu, T., 2005, Density functional theory study of the FT-IR spectra of phthalimide and N-bromophthalimide, Spectrochimica, Acta Part A, 62(4-5), 918–925. <https://doi.org/10.1016/j.saa.2005.02.051>.
- [31] Sundaraganesan, N., Saleem, H., Mohan, S., Ramalingam, M., & Sethuraman, V., 2005, FTIR, FT-Raman spectra and ab initio DFT vibrational analysis of 2-bromo-4-methyl-phenylamine, Spectrochimica Acta Part A, 62(1-3), 740–751. <https://doi.org/10.1016/j.saa.2005.02.043>.
- [32] Singh, S.J., & Pandey, S.M., 1974, Molecular Structure and vibrational analysis of 1-bromo-2-chlorobenzene using ab initio HF and density functional theory (B3LYP) calculations. Indian J Pure Appl Phys, 12, 300–304.
- [33] Varsanyi, G., 1973, Assignments for vibrational spectra of seven hundred benzene derivatives, vols.1 and 2, Academic kiado, Budapest.
- [34] Jag, M., 2001, Organic Spectroscopy-Principles and Applications, 2nd ed, Narosa publishing House, New Delhi.
- [35] Bharanidharan, S., Saleem, H., Subashchandrabose, S., Suresh, M., Ramesh Babu, N., 2017, FT-IR, FT-Raman and UV-Visible Spectral analysis on (E)-N²-(thiophene-2-ylmethylene) Nicotinohydrazide, Archives in Chemical Research, 1 (2:7) 1-14, <https://doi.org/10.21767/2572-4657.100007>.
- [36] Sathyanarayanan, D.N., 2004, Vibrational Spectroscopy theory and applications, New Age International Publishers, New Delhi, 2004, 446–447.
- [37] Roeges, N.P.G., 1994, A Guide to the complete interpretation of Infrared Spectra of Organic structure, Wiley, New York.
- [38] Barthes, M., De Nunzio, G., & Ribet, M., 1996, Polarons or proton transfer in chains of peptide groups? Synthetic Metals, 76(1-3), 337–340. [https://doi.org/10.1016/0379-6779\(95\)03484-2](https://doi.org/10.1016/0379-6779(95)03484-2).
- [39] James, C., Ravikumar, C., Sundius, T., Krishnakumar, V., Kesavamoorthy, R., Jayakumar, V.S., & Hubert Joe, I., 2008, FT-Raman and FTIR spectra, normal coordinate analysis and ab initio computations of (2-methylphenoxy)acetic acid dimer. Vib. Spectrosc., 47(1), 10–20. <https://doi.org/10.1016/j.vibspec.2008.01.006>.
- [40] Singh, D.K., Srivastava, S.K., Ojha, A.K., & Asthana, B.P., 2008, Vibrational study of thiophene and its solvation in two polar solvents, DMSO and methanol by Raman spectroscopy combined with ab initio and DFT calculations, J. Mol. Struct., 892(1-3), 384–391. <https://doi.org/10.1016/j.molstruc.2008.06.008>.
- [41] Fleming, G.D., Koch, R., & Campos Vallete, M.M., 2006, Theoretical study of the syn and anti thiophene-2-aldehyde conformers using density functional theory and normal coordinate analysis, Spectrochim. Acta A, 65(3-4), 935–945. <https://doi.org/10.1016/j.saa.2006.01.038>.
- [42] Badawi, H.M., 2009, Structural stability, C–N internal rotations and vibrational spectral analysis of non-planar phenylurea and phenylthiourea, Spectrochim. Acta A, 72(3), 523–527, <https://doi.org/10.1016/j.saa.2008.10.042>.
- [43] Lorenc, J. (2012). Dimeric structure and hydrogen bonds in 2-N-ethylamino-5-methyl-4-nitro-pyridine studied by XRD, IR and Raman methods and DFT calculations, Vib. Spectrosc. 61, 112–123. <https://doi.org/10.1016/j.vibspec.2012.03.006>.
- [44] Socrates, G., 1980, Infrared Characteristic Group Frequencies, John Wiley and Sons Ltd, New York.
- [45] Subashchandrabose, S., Meganathan, C., Erdoğan, Y., Saleem, H., Jajkumar, C., & Latha, P., 2013, Vibrational and conformational analysis on-N1-N2-bis (pyridine-4-yl) methylene benzene-1, 2-diamine, J. Mol. Struct., 1042, 37–44. <https://doi.org/10.1016/j.molstruc.2013.03.034>.
- [46] Silverstein, M. Basseller, C.G., Morill, C., 1981, Spectrometric identification of organic compound”, John Wiley; Network.
- [47] Lorenc, J., 2012, Dimeric structure and hydrogen bonds in 2-N-ethylamino-5-methyl-4-nitro-pyridine studied by XRD, IR and Raman methods and DFT calculations, Vib. Spectrosc. 61, 112–123. <https://doi.org/10.1016/j.vibspec.2012.03.006>.
- [48] Ramesh Babu, N., Subashchandrabose, S., Syed Ali Padusha, M., Saleem, H., & Erdoğan, Y., 2014, Synthesis and spectral characterization of hydrazone derivative of furfural using experimental and DFT methods. Spectrochimica Acta A, 120, 314–322. <https://doi.org/10.1016/j.saa.2013.09.089>.
- [49] Goresky, S.I., 2013, SWizard Program Revision 4.5, University of Ottawa, Ottawa, Canada.
- [50] Chamberlain, N.F., 1974, the Practice of NMR Spectroscopy with Spectra-Structure Correlations for Hydrogen-1, Plenum Press.
- [51] Andraud, C., Brotin, T., Garcia, C., Pelle, F., Goldner, P., Bigot, B., & Collet, A., 1994, Theoretical and experimental investigations of the nonlinear optical properties of vanillin, polyvanillin, and bisvanillin derivatives. J. Am. chem. Soc. 116(5), 2094–2102. <https://doi.org/10.1021/ja00084a055>.

- [52] Geskin, V.M., Lambert, C., & Brédas, J.L., 2003, Origin of High Second- and Third-Order Nonlinear Optical Response in Ammonio/BoratoDiphenylpolyene Zwitterions: the Remarkable Role of Polarized Aromatic Groups, *J. Am. Chem. Soc.* 125(50), 15651–15658. <https://doi.org/10.1021/ja035862p>.
- [53] Liu, J., Chen, Z., & Yuan, S., 2005, Study on the prediction of visible absorption maxima of azobenzene compounds, *J. Zhejiang Univ. Sci.* 6B(6), 584–589. <https://doi.org/10.1631/jzus.2005.B0584>.
- [54] James, C., Raj, A.A., Reghunathan, R., Jayakumar, V.S., & Joe, I.H., 2006, Structural conformation and vibrational spectroscopic studies of 2,6-bis(p-N,N-dimethyl benzyldiene) cyclohexanone using density functional theory, *J. Raman Spectrosc.* 37(12), 1381–1392. <https://doi.org/10.1002/jrs.1554>.
- [55] Liu, J.N., Chen, Z.R., & Yuan, S.F., 2005, Study on the prediction of visible absorption maxima of azobenzene compounds. *Journal of Zhejiang University. Science. B*, 6(6), 584. <https://doi.org/10.1631/jzus.2005.B0584>.
- [56] Kohn, W., Becke, A.D., & Parr, R.G., 1996, Density Functional Theory of Electronic Structure, *J. Phys. Chem.* 100(31), 12974–12980. <https://doi.org/10.1021/jp960669l>.
- [57] Parr, R.G., & Pearson, R.G., 1983, Absolute hardness: companion parameter to absolute electronegativity, *J. Am. Chem. Soc.* 105(26), 7512–7516. <https://doi.org/10.1021/ja00364a005>.
- [58] Politzer, P., & Abu-Awwad, F., 1998, A comparative analysis of Hartree-Fock and Kohn-Sham orbital energies, *Chem. Acc.* 99(2), 83–87. <https://doi.org/10.1007/s002140050307>.
- [59] Gunasekaran, S., Kumaresan, S., Arunbalaji, R., Anand, G., & Srinivasan, S., 2008, Density functional theory study of vibrational spectra, and assignment of fundamental modes of dacarbazine, *J. Chem. Sci.* 120(3), 315–324. <https://doi.org/10.1007/s12039-008-0054-8>.
- [60] Bevan Ott, J., Boerio-Goates, J., 2000, *Calculations from Statical Thermodynamics*, Academic Press.